Proceedings of the 29th Annual International
Conference of the IEEE EMBS
Cité Internationale, Lyon, France
August 23-26, 2007.

Calibrating an Ultrasonic Computed Tomography System Using a Time-of-Flight Based Positioning Algorithm

Adam Filipik, Igor Peterlik, Dusan Hemzal, Jiri Jan, Radovan Jirik, Michael Zapf, Nicole Ruiter

***Abstract* — This paper presents a method for geometrical and time-delay auto-calibration of an ultrasonic computed tomography (USCT) system. The algorithms used for the calibration are based on the principles similar to the global positioning system (GPS) navigation. Ultrasonic transmitters and receivers in USCT can be viewed like satellite transmitters and mobile receiver units in GPS. However, unlike in GPS, none of the positions of the transmitters or receivers in USCT are assumed to be known and all are the to-be-calibrated unknowns. The presented method is capable of calibrating the positions of all ultrasonic transducers and their individual time delays at once. No calibration phantoms are necessary.**

I. Introduction

Ultrasonic Computed Tomography (USCT) is an imaging modality currently under development. It is primarily aimed at breast cancer diagnosis. The imaged object is placed in a tank filled with water as a coupling medium, and surrounded with several thousands of ultrasonic transducers. Each of these transducers is used for either transmitting (sender) or receiving (receiver) ultrasonic pulses. The recorded signals, so called A-scans (Figure 2), can then be used for reconstruction of tomographic images of the object [1][6].

A 3D setup for USCT is currently developed at Forschungszentrum Karlsruhe (FZK), Germany [1]. The system (Figure 1) consists of 384 senders and 1536 receivers mounted on 48 exchangeable transducer array systems (TAS). The cylinder which holds the TASes can be rotated in 6 steps to achieve a total of 11,520 virtual transducers, which can produce approximately 3.5 million A-scans. The transducers' mean frequency is 2.7 MHz and the A-scan signals are sampled at 10MHz. A complete system scan produces about 20GB of data.

For the reconstruction of tomographic images, it is crucial to know the positions of individual transducers accurate within the order of a wavelength. An estimate of the positions can be made based on the dimensions of the TASes and the cylinder to which they are fixed. But even small positioning errors (in the range of tenths of millimeters) can lead to significant degradation of image quality. With respect to the number of transducers in the system, it is impractical to measure the distances between them manually.

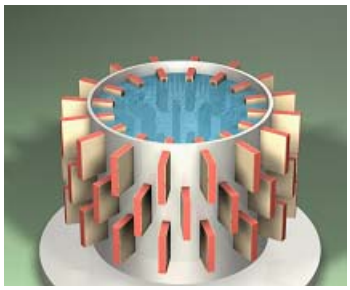

Figure 1: A drawing of the 3D USCT device developed in FZK, Karlsruhe, Germany.

We propose an auto-calibration technique, which utilizes only the internal ultrasonic signals produced by the system to solve the calibration problem. The technique is based on the same principles as the GPS navigation. Essentially, the ultrasonic signals and particularly the time-of-arrivals of individual ultrasonic pulses are used for a triangulation. The triangulation is formulated as a minimization problem, where the to-be-minimized quantity is the sum of squares of differences between a measured and an estimated pulse arrival time. The unknown minimization parameters are the positions and individual time-delays of transducers.

A similar approach can be seen in the calibration of an underwater ultrasound imaging system [2]. Here, the authors relied on the presence of a high precision positioning device with an attached hydrophone. The knowledge of the transmitting hydrophone positions provides a reference coordinate system to the calibration, just like in GPS, where the orbits of the satellites can be very accurately calculated. In our approach, however, the positioning device is not needed, and all positions and time delays (both the senders and receivers) are the unknown parameters. Also, there is no need for any sender-to-sender and receiver-to-receiver distances to be known.

II. The USCT Calibration Method

For the USCT calibration, a so-called empty measurement has to be made. In such a measurement, the tank is filled only with water. Each sender is excited to produce an ultrasonic pulse wave, which travels through the water and reaches all receiving transducers. Each of the receivers records an A-scan signal (Figure 2). The complete measurement consists of consecutively firing all senders

Manuscript received March 31, 2007. This project is sponsored by the National research centre DAR (Ministry of Education, Czech Republic, project no. 1M6798555601). It is further supported by the DAAD grant no. D12-CZ9/07-08, and partially also by the research frame of the FEEC BUT (Ministry of Education, Cz. Rep., project no. MSM 0021630513).

A. Filipik, J. Jan, and R. Jirik are with the Dept. Of Biomedical Eng., FEEC, Brno University of Technology, Czech Republic (corresp. author J. Jan, jan@feec.vutbr.cz), I. Peterlik is with the Faculty of Informatics, Masaryk University, Brno, Czech Republic, D. Hemzal is with the Dept. of Condensed Matter Physics, Masaryk University Brno, Czech Republic, M. Zapf, N. Ruiter are with the Institute for Data Processing and Electronics (IPE) in Forschungszentrum, Karlsruhe, Germany.

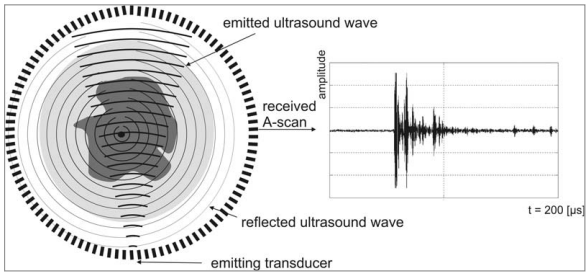

Figure 2: The USCT system (a view from the top)

(one sender at a time).

In each A-scan, several pulses can be detected. The first corresponds to the direct path of the ultrasound wave from the sender to the receiver, whereas later pulses correspond to paths with reflections from the tank walls or the water surface. By detecting the position of the first pulse, we obtain a so called time-of-arrival value ($TOA_{s,r}$) for a particular sender-receiver combination. The time-of-arrival can be expressed as a function of sender and receiver positions and time-delays, which are introduced by the electronics processing the signals on both sides:

$$TOA_{s,r} = TOF_{s,r} + \tau_s + \tau_r + \varepsilon_{s,r} \quad (1)$$

$$TOF_{s,r} = r_{s,r} / v = \sqrt{(x_s - x_r)^2 + (y_s - y_r)^2 + (z_s - z_r)^2} / v \quad (2)$$

where, $TOF_{s,r}$ is the time-of-flight of the pulse from sender s to receiver r, τ_s and τ_r are the sender and receiver time delays, ε is the measurement noise, $r_{s,r}$ is the distance from the sender to the receiver, v is the actual speed of sound, and x_s, y_s, z_s and x_r, y_r, z_r are the position coordinates of the sender and the receiver, respectively.

Equations (1) and (2) are very similar to the so-called pseudorange equations used in GPS [3], where the time delay components are analogical to the satellites' and receivers' clocks offsets. There is a major difference, though, in the fact that in the USCT, neither the sender nor the receiver positions and delays are assumed to be known. The only known parameter is the speed of sound in water v, which can be very accurately calculated if the temperature is known [4].

Similarly as in the case of GPS, we can solve for the unknown positions and delays using a nonlinear least squares approach which minimizes the sum of squares of differences between the measured and estimated time-of-arrivals. For this we need to introduce a set of initial position and delay estimates (sender: $x_{s,0}$, $y_{s,0}$, $z_{s,0}$, $\tau_{s,0}$ and receiver: $x_{r,0}$, $y_{r,0}$, $z_{r,0}$, $\tau_{r,0}$) and estimate-errors (sender: Δx_s, Δy_s, Δz_s, $\Delta\tau_s$ and receiver: Δx_r, Δy_r, Δz_r, $\Delta\tau_r$). The correct positions and delays are then given by the sums:

$$\{x_s, y_s, z_s, \tau_s\} = \{x_{s,0} + \Delta x_s, y_{s,0} + \Delta y_s, z_{s,0} + \Delta z_s, \tau_{s,0} + \Delta\tau_s\}$$

$$\{x_r, y_r, z_r, \tau_r\} = \{x_{r,0} + \Delta x_r, y_{r,0} + \Delta y_r, z_{r,0} + \Delta z_r, \tau_{r,0} + \Delta\tau_r\}$$

By substituting the above into (2) and expanding it into a Taylor series (up to the 1st order) we obtain a linearized approximation of the time-of-flight values (3) (see bellow), where

$$d_{s,r,0} = \sqrt{(x_{s,0} - x_{r,0})^2 + (y_{s,0} - y_{r,0})^2 + (z_{s,0} - z_{r,0})^2}$$

is the sender-receiver distance estimate. By substituting (3) back into (1) we can formulate the overall difference between the estimated and detected time-of-arrival of each pulse (4) (see bellow).

We can now arrange a set of equations (4) (one for each sender - receiver combination) into a matrix representation:

$$\boldsymbol{J}\Delta\boldsymbol{x} = \boldsymbol{r}, \quad (5)$$

where $\Delta\boldsymbol{x} = [\Delta x_{s1}, \Delta y_{s1}, \Delta z_{s1}, \Delta\tau_{s1} \ldots \Delta x_{sN}, \Delta y_{sN}, \Delta z_{sN}, \Delta\tau_{sN}, \Delta x_{r1}, \Delta y_{r1}, \Delta z_{r1}, \Delta\tau_r, \ldots \Delta x_{rM}, \Delta y_{rM}, \Delta z_{rM}, \Delta\tau_{rM}]^T$ is the vector of the unknown estimate-error components,

$\boldsymbol{r} = [\Delta TOA_{s1,r1} \ldots \Delta TOA_{s1,rM}, \Delta TOA_{s2s,r1} \ldots \Delta TOA_{sNs,rM}]^T$ is the vector of time-of-flight residuals (differences of estimated and detected TOAs), and $\boldsymbol{J}$ is the system matrix consisting of the first-order Taylor series components (the fractions on the right side of (4)). Note that $\boldsymbol{J}$ is actually a Jacobian matrix as its cells are equal to the partial derivatives of the $TOA_{s,r}$ functions.

In order to obtain the vector of the unknown sender and receiver positions and delays

$\boldsymbol{x} = [x_{s1}, y_{s1}, z_{s1}, \tau_{s1} \ldots x_{sN}, y_{sN}, z_{sN}, \tau_{sN}, x_{r1}, y_{r1}, z_{r1}, \tau_{r1} \ldots x_{rM}, y_{rM}, z_{rM}, \tau_{rM}]^T$,

we can repeatedly solve the linearized overdetermined system in the least mean squares sense:

$$\Delta\boldsymbol{x}_k = (\boldsymbol{J}_k^T \boldsymbol{J}_k)^{-1} \boldsymbol{J}_k^T \boldsymbol{r}_k \quad (6)$$

where ^{T} denotes transpose, $^{-1}$ matrix inversion, and k is the iteration number. After each iteration, the vector of estimate values is updated:

$$\boldsymbol{x}_{k+1} = \boldsymbol{x}_k + \Delta\boldsymbol{x}_k \quad (7)$$

For the next solution of (6), the new estimate (7) is used to calculate the residual $\boldsymbol{r}_{k+1}$ and the Jacobian $\boldsymbol{J}_{k+1}$. Note that the above iteration scheme is actually equivalent to the Gauss-Newton method, in which the product of the Jacobians $\boldsymbol{J}^T\boldsymbol{J}$ (as in (6)) is used to approximate a generally nonlinear Hessian matrix $\boldsymbol{H}$, and any higher order terms are neglected. This approximation is very efficient but is only valid if the first estimate of unknowns is close enough to the correct solution and the residuals are close to being linear (at the estimate point) [5]. If that is not the case, the Gauss-Newton method might diverge, and it is better to use the Levenberg-Marquardt method which is a blend of the Gauss-Newton and the gradient descent methods. For the

$$TOF_{s,r} = \sqrt{(x_{s,0} + \Delta x_s - x_{r,0} - \Delta x_r)^2 + (y_{s,0} + \Delta y_s - y_{r,0} - \Delta y_r)^2 + (z_{s,0} + \Delta z_s - z_{r,0} - \Delta z_r)^2} / v$$
$$\cong \frac{d_{s,r,0}}{v} + \frac{x_{s,0} - x_{r,0}}{v d_{s,r,0}} \Delta x_s - \frac{x_{s,0} - x_{r,0}}{v d_{s,r,0}} \Delta x_r + \frac{y_{s,0} - y_{r,0}}{v d_{s,r,0}} \Delta y_s - \frac{y_{s,0} - y_{r,0}}{v d_{s,r,0}} \Delta y_r + \frac{z_{s,0} - z_{r,0}}{v d_{s,r,0}} \Delta z_s - \frac{z_{s,0} - z_{r,0}}{v d_{s,r,0}} \Delta z_r \quad (3)$$

$$\Delta TOA_{s,r} = \frac{x_{s,0} - x_{r,0}}{v d_{s,r,0}} \Delta x_s + \frac{y_{s,0} - y_{r,0}}{v d_{s,r,0}} \Delta y_s + \frac{z_{s,0} - z_{r,0}}{v d_{s,r,0}} \Delta z_s + \Delta\tau_s - \frac{x_{s,0} - x_{r,0}}{v d_{s,r,0}} \Delta x_r - \frac{y_{s,0} - y_{r,0}}{v d_{s,r,0}} \Delta y_r - \frac{z_{s,0} - z_{r,0}}{v d_{s,r,0}} \Delta z_r + \Delta\tau_r \quad (4)$$

Levenberg-Marquardt method, the estimate is iteratively updated by

$$\Delta \mathbf{x}_k = (\boldsymbol{J}^T\boldsymbol{J} + \lambda diag[\boldsymbol{J}^T\boldsymbol{J}])^{-1}\mathbf{J}_k{}^{\mathrm{T}}\mathbf{r}_k \qquad (8)$$

where λ is a parameter controlling the inclination of the method either towards the Gauss-Newton solution or towards the gradient descent. λ is some small number greater than zero, and is chosen heuristically [5].

III. Numerical Analysis

In order to solve the nonlinear problem by either of the two methods, we have to introduce some constraints otherwise it will not converge. We are trying to find the positions and delays of the transducers based only on the measurements of their relative distances, in the lack of any reference (as defined by the known positions of satellites in the GPS case), which would give some information on the position and orientation of the USCT transducers relative to a coordinate system. If we suppose one correct solution of the equation system (the correct positions of all transducers) we could translate or rotate these positions (all at once) in any direction and under any angle and still obtain a correct solution of this equation system. Even though the system is heavily overdetermined (the ratio of number of equations to the number of unknowns is in hundreds), the system is rank deficient (6 less than full rank – one for each degree of freedom) and has therefore an infinite number of correct solutions.

We can constrain the system to yield one possible solution by introducing virtual "anchors". In many calibration techniques, anchors are typically referred to as nodes of known positions – reference points. Although we are not sure where our transducers lie, we can simply set (anchor) the position of one transducer s_1 to an unchangeable value (for example into the origin of the coordinate system: s_1:{0,0,0}). We can do this by setting the x, y, and z coordinates of s_1 to zero in the first estimate $\boldsymbol{x_0}$. To insure that the position of s_1 is not altered by the least squares solution, we must add an equation, one for each coordinate, expressing the stability of the solution with respect to each error component of s_1: $\Delta x_{s1} = 0$, $\Delta y_{s1} = 0$, $\Delta z_{s1} = 0$. This can easily be done by adding 3 rows to the Jacobian matrix with all components equal to zero except those matching x, y and z error components of s_1.

Now, if we imagine the correct positions of the transducers again (having in mind, that we have anchored one transducer to a fixed position) we cannot translate the USCT system anymore, but we still can rotate it about this anchor point. Therefore, other transducers should be anchored. But by anchoring another transducer to a particular position we introduce a systematic error, because the correct position is not known. Instead we anchor only two out of the three coordinates s_2:{x_{const}, y_{const}, z}. This way the distance between s_1 and s_2 can still be adjusted by solving the least squares problem, but the overall variability of the rest of the transducers is constrained at the same time. To stabilize the solution completely, we need to choose one more transducer, and anchor the remaining variable coordinate of s_2, s_3:{x, y, z_{const}}. The anchoring can also be seen as choosing one particular coordinate system (out of an infinite number of possible systems) in which we solve the calibration problem.

IV. Simulation Results

In order to verify the method, a simulation study was done consisting of setting up a virtual model of the USCT system. 64 senders and 128 receivers were taken into consideration (about 1/10 of the actual numbers). This resulted in (64 + 128) 4 = 768 unknown parameters (3 position coordinates and 1 delay each) and $64 \cdot 128 = 8192$ independent TOA measurements. The simulation was carried out in Matlab. To solve the matrix inversions in the least squares problem (5), the QR-decomposition with pivoting (implemented in the Matlab's backslash operator) was used.

At first, the size of the convergence region was tested. The initial estimate values were derived from the set of simulated ground truth position- and delay values by introducing an estimate error of various magnitudes. The process of solving for the unknowns iterated 15 times. Noise-less measurement was assumed at first. The results can be seen in Figure 3. The convergence region is surprisingly large – in the magnitude of the diameter of the USCT system (20 cm). This means that in the absence of noise, a large error in the first estimate is acceptable. The error minimum is limited by the used data type (Matlab's double-precision floating point). Both the Gauss-Newton (6) and the Levenberg-Marquardt (8) methods yielded almost identical results.

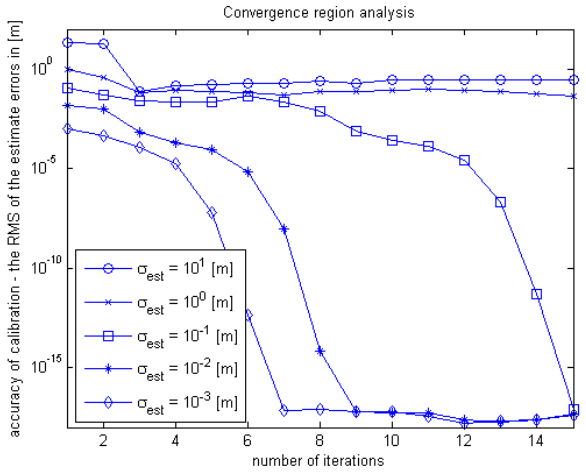

Figure 3: Convergence region analysis. The plot shows the calibration accuracy (RMS of the estimate errors) for different starting estimates. The standard deviation of the initial estimates is given in the legend (in meters). No measurement noise is assumed. The vertical axis represents the accuracy of the calibration (in meters); the horizontal axis gives the number of iterations.

The second part of the simulation consisted in the introduction of measurement noise, i.e. the inaccuracy of the pulse detection was included into the model. It can be seen (Figure 4) that in order to satisfy the needs of the USCT reconstruction (transducer position accuracy within a tenth of a millimeter), the pulses must be detected with an error under 10^{-7}s (corresponding to 1/3 of the wavelength in the current setup). Again both methods (6) and (8) produced very similar results.

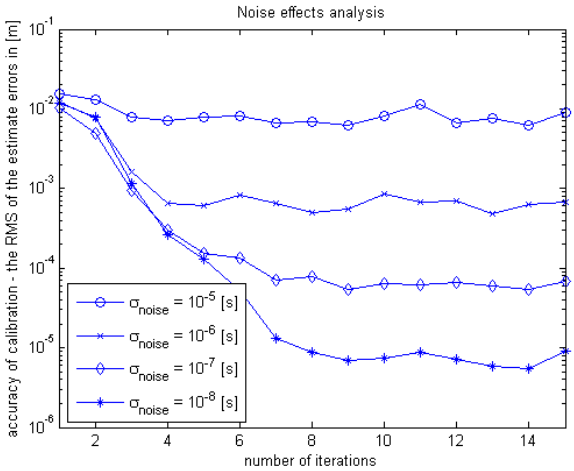

Figure 4: Noise effects analysis. This plot shows the calibration accuracy (RMS of the estimate errors) for different values of measurement noise (pulse detection inaccuracies). The standard deviation of the inaccuracies is given in the legend in seconds. The accuracy of the starting estimate is 10^{-2} m. The vertical axis represents the accuracy of the calibration (in meters); the horizontal axis gives the number of iterations.

The outcome of the simulated USCT calibration can be seen in Figure 5, where the positions of individual transducers are shown in 3D scatter plots. It can be seen that the calibrated transducers are equally distributed on the surfaces of the TASes forming a cylindrical outline of the USCT tank, as it was modeled in the simulation (only every second TAS from the top TAS layer was part of the model). The first estimate had an RMS error of $\sigma = 10^{-2}$ m, and the measurement noise standard deviation was $\sigma = 10^{-7}$ s. Although the fit to the ground-truth is not perfect, the differences are too small (compared to the overall dimensions) to be seen.

V. Conclusion

A new method was developed for the calibration of a USCT system. For its flexibility, the GPS navigation principle was used as a resource for our method. The main extension over GPS is that neither the transducers nor the receivers are assumed to be in known positions and all are calibrated at once. The calibration is self-contained – no additional calibration phantoms, high precision positioning devices, etc, are needed. The accuracy of the calibration is primarily limited by the accuracy of the signal detection.

In the near future, we plan to evaluate the method on real USCT data.

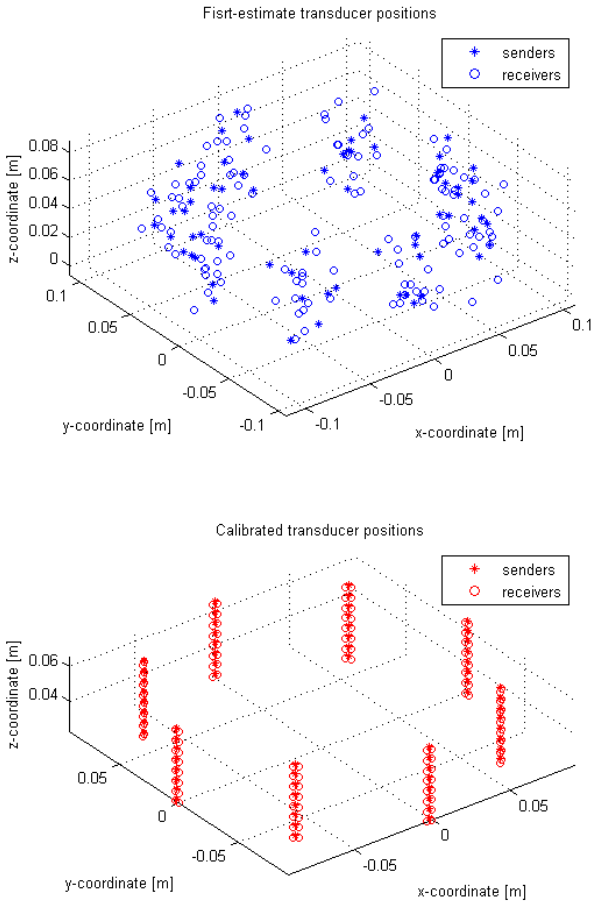

Figure 5: Two 3D scatter plots with positions of individual transducers before (top) and after calibration (bottom).

VI. Acknowledgment

Authors sincerely acknowledge the contribution of Dr Rainer Stotzka of Forschungszentrum Karlsruhe Germany, who was one of the authors of the experimental USCT system, and substantially contributed to discussions on the merit of the research in its initial phases.

References

[1] Ruiter, N.V., Schwarzenberg, G.F., Zapf M., Liu R., Stotzka R., Gemmeke H., *3D Ultrasound Computer Tomography: Results with a Clinical Breast Phantom*, IEEE Symposium Ultrasonics 2006.

[2] Yue Li, "Position and Time-Delay Calibration of Transducer Elements in a Sparse Array for Underwater Ultrasound Imaging", *IEEE Transaction on Ultrasonics, Feroelectrics, and Frequency Control*, Vol. 53, No.8, Aug. 2006.

[3] Hofmann-Wellenhof, B., Lichtenegger, H., and Collins, J., *GPS: Theory and Practice*, 2001, Springer-Verlag Wien.

[4] Bamber J.C., Hill C.R, *Physical Principles of Medical Ultrasonics*, John Wiley and Sons, 2004.

[5] Press, W. H. et al.: *Numerical Recipes in C, The Art of Scientific Computing (Second edition)*, Cambridge University Press, 2002.

[6] Jiřík R., Stotzka R., Taxt T. (2005): 'Ultrasonic Attenuation Tomography Based on Log-Spectrum Analysis,' Proceedings of SPIE, Medical Imaging 2005. Volume: 5750, 2005.